Reaction-Diffusion based Autonomous Control of Camera Sensor Networks

Katsuya Hyodo
Graduate School of Information Science and Technology, Osaka University
1-5 Yamadaoka, Suita, Osaka 565-0871, Japan
k-hyodo@ist.osaka-u.ac.jp

Naoki Wakamiya
Graduate School of Information Science and Technology, Osaka University
1-5 Yamadaoka, Suita, Osaka 565-0871, Japan
wakamiya@ist.osaka-u.ac.jp

Masayuki Murata
Graduate School of Information Science and Technology, Osaka University
1-5 Yamadaoka, Suita, Osaka 565-0871, Japan
murata@ist.osaka-u.ac.jp

ABSTRACT

Taking into account requirements of sensor networks, we need fully-distributed and self-organizing control mechanisms which are scalable to the size of a network, robust to failures of sensor nodes, and adaptive to different and dynamically changing topology and changes in wireless communication environment. Moreover, a particular problem for camera sensor networks is that in sending video data to data gathering centers in real-time, nodes must adjust video coding rate in consideration of the high volume of video data against the network capacity. To accomplish both of the above two goals, our research group focuses on behavior of biological systems, which inherently are scalable, adaptive, and robust. In this paper, we propose an autonomous rate control mechanism based on a reaction-diffusion model for remote surveillance or tracking applications. Through local interactions among neighboring sensor nodes, each node sets its coding rate appropriate for the location of targets and the local network capacity. We conducted simulation experiments on small-size and large-size camera sensor networks, and verified the effectiveness of our proposed mechanism.

Categories and Subject Descriptors

C.2.4 [COMPUTER-COMMUNICATION NETWORKS]: Distributed Systems—Distributed applications

General Terms

Algorithms, Experimentation

Keywords

Camera sensor networks, Reaction diffusion, Biological system

1. INTRODUCTION

BIONETICS 2007 December 10-12, 2007, Budapest, Hungary

Sensor network is one of the most promising and key technologies for safe, secure, and comfortable society. By distributing a large number of sensor nodes and organizing a network through wired and/or wireless communication, one can obtain detailed information about surroundings, remote region, and objects. In particular, camera sensor networks, which are composed of nodes equipped with a camera, are useful in a variety of applications such as remote surveillance, home security, and tracking applications [1].

Generally, control mechanisms for sensor networks must be scalable, adaptive, and robust, because of a large number of sensor nodes, random or unplanned deployment, and dynamic topology changes due to addition, movement, and removal of sensor nodes. In addition, due to difficulty in managing a large number of nodes in a centralized manner, mechanisms must be fully distributed and self-organizing. Moreover, a particular problem for camera sensor networks is transmission of high volume traffic of video data over a wireless network of limited capacity. Therefore, in sending video data to data gathering centers in real-time, nodes must adjust the video coding rate taking into account the network capacity and the importance of video data. In a case of surveillance or monitoring applications, video data obtained at a camera, which detects and tracks a suspicious or interesting object, should have the sufficiently high resolution and high quality to have a better look at the target.

To accomplish the above mentioned goals in a wireless sensor network, we adopt a reaction-diffusion model in this paper. A reaction-diffusion equation was first proposed by Alan Turing as a mathematical model for pattern generation on the surface of body of fishes and mammals [6] . In a reaction-diffusion model, through local interactions among molecules of neighboring cells, a variety of patterns of morphogen concentrations emerge in a self-organizing manner. Autonomously generated patterns can be used for routing, clustering, scheduling, and topology control on sensor networks [2, 3, 4, 7]. Our early work on a reaction-diffusion based control mechanisms for a sensor network [4] verified the practicality of reaction-diffusion based pattern formation on a wireless sensor network through experiments and two acceleration schemes for faster pattern generation were proposed. In smart sensor networks for a forest fire application, a stripe pattern is organized from a robot load point to a fire control point through local and mutual inter-

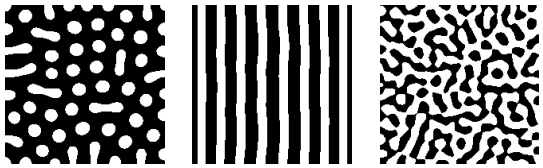

(a) spots (b) stripes (c) maze

Figure 1: Example of generated patterns

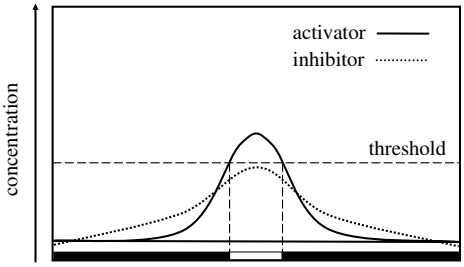

Figure 2: Pattern generation

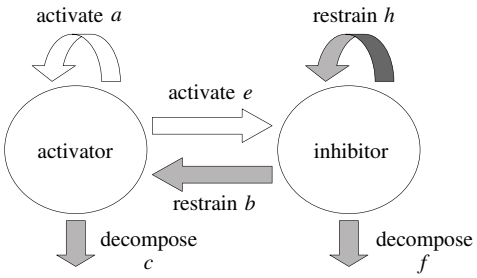

Figure 3: Reaction of two morphogens

actions among distributed sensor nodes and mobile robots walk along the stripe to fight a fire [2]. RDMAC [3] is a reaction-diffusion based MAC protocol, where they noticed the similarity among a scheduling pattern of spatial TDMA and a spot pattern of leopards. A node inhibits packet emission of neighboring nodes in its range of radio signals while encouraging nodes out of the range to send packets for better spatial use of a wireless channel. For camera sensor networks, a cooperative control model for a surveillance system which consists of plural Pan-Tilt-Zoom cameras and having no central control unit is proposed [7]. Each camera adjusts their observation area to decrease blind spots in the whole surveillance area by control algorithms based on a reaction-diffusion model.

In this paper, we propose an autonomous mechanism based on a reaction-diffusion model for coding rate control in camera sensor networks for remote surveillance and tracking applications. Specifically, we generate spot patterns so that the morphogen concentrations have a peak at a camera detecting a target in its observation area. In addition, to prepare cameras in the direction of a moving target for future detection, their video coding rates, in other words, their morphogen concentrations are made slightly higher than others. As a result, we see a pattern of concentric circles for a stationary target and an elliptic pattern for a moving target. Furthermore, we also propose a mechanism to keep the total of coding rate low for closely located targets considering the limited capacity of a wireless network. Through simulation experiments, we verified the effectiveness of our proposed mechanism.

The rest of the paper is organized as follows. In Section 2, we introduce a pattern generation mechanism by a reaction-diffusion model that our paper is based on. Next in Section 3, we describe our reaction-diffusion based control mechanism for camera sensor networks. In Section 4, we then show and discuss results of simulation experiments. Finally, we conclude the paper in Section 5.

2. PATTERN FORMATION BY REACTION-DIFFUSION EQUATION

Generally, pattern generation in a reaction-diffusion model is based on interactions among two virtual morphogens, i.e., activator and inhibitor. Reaction and diffusion of the two morphogens make spatial heterogeneity of their concentrations, i.e., a pattern. Depending on the form of reaction-diffusion equations and their parameters, a variety of patterns can be generated as illustrated in Fig. 1. Since we want to generate spot patterns where spots correspond to targets, we apply the following reaction-diffusion equation.

$$\begin{cases} \dfrac{\partial u}{\partial t} = F(u,v) + D_u \nabla^2 u - du + E(t) \\ \dfrac{\partial v}{\partial t} = G(u,v) + D_v \nabla^2 v - gv, \end{cases} \tag{1}$$

where u and v are concentrations of activator and inhibitor, respectively. The first term of the right-hand side is a reaction team and the second term is a diffusion term. F and G are nonlinear functions for reactions. D_u and D_v are the diffusion rate of activator and inhibitor, respectively. d and g are parameters for decomposition or decrease of morphogens per unit time. ∇^2 is the Laplacian operator. $E(t)$ is the amount of stimulus.

The following two conditions must be satisfied to generate patterns; 1) activator activates itself and inhibitor, whereas inhibitor restraints itself and activator, and 2) inhibitor diffuses faster than activator ($D_v > D_u$). A mechanism of pattern generation can be explained as follows. In Fig. 2, those hypothetical chemicals are arranged in a line on the x-axis. The y-axis corresponds to the concentrations of activator and inhibitor. Now, consider that the concentration of activator has a peak at the center by a slight perturbation. The concentrations of activator and inhibitor are both increased around the peak by self-activation. The generated inhibitor diffuses faster than the activator and restrains generation of activator at further regions. On the other hand at the peak, the concentration of activator is kept higher than that of inhibitor for slower rate of diffusion. Consequently, the diversity in the concentration of activator emerges and a pattern appears. For example, when we color a point where the concentration of activator exceeds a certain threshold with white and others with black, we can see a black-white-black pattern shown at the bottom of Fig. 2.

Figure 3 illustrates reactions of morphogens following the

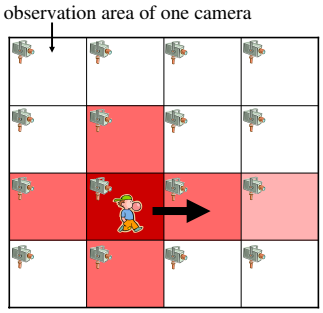

Figure 4: Camera sensor network

functions F and G below.

$$\begin{cases} F(u,v) = \max\{0, \min\{au - bv - c, M\}\} \\ G(u,v) = \max\{0, \min\{eu - hv - f, N\}\}, \end{cases} \quad (2)$$

where a and e correspond to the rate of activation and b and h are for inhibition. c and f are parameters for decrease of morphogens per unit time. M and N are constants of limit.

These parameters must satisfy the following conditions to generate a pattern centered at a point where stimulus $E(t) > 0$ exists [5].

$$\frac{a-d}{b}\frac{f}{e} - \frac{c}{b} \leq 0 \quad \text{and} \quad \frac{a-d}{b}\frac{M}{d} - \frac{c}{b} < \min\{\frac{e}{h+g}(\frac{M}{d} - \frac{f}{e}), \frac{N}{g}\} \quad (3)$$

or

$$a - d > h + g \quad \text{and} \quad \frac{a-d}{b}\frac{M}{d} - \frac{c}{b} < \min\{\frac{e}{h+g}(\frac{M}{d} - \frac{f}{e}), \frac{N}{g}\} \quad (4)$$

As can be seen, the parameter setting does not depend on system conditions such as the size of region.

3. REACTION-DIFFUSION BASED CONTROL OF CAMERA SENSOR NETWORKS

Figure 4 illustrates a surveillance or monitoring system that we consider in this paper. Each square corresponds to the observation area of a camera sensor node. The darker the square is, the higher the video coding rate is. We assume that nodes are arranged in a grid topology, considering town or room monitoring as an application of the mechanism. For example in a town, we can consider such a scenario where camera sensor nodes are placed at intersections. A node can communicate with four neighbors in up, right, down, and left directions. Nodes at a corner of the monitoring region have two neighbors and nodes at an edge have three neighbors. The assumption on node layout can be relaxed by adapting a numerical solution technique for ∇^2 (details are not shown for space limitation).

Each node has a camera and a wireless communication device. A camera or a node has the capability of object recognition and motion detection with which the existence, speed, and direction of a target in its observation area.

3.1 Basic behavior

Basically, at regular control intervals of T seconds, each node calculates the reaction-diffusion equation by using the information it received in the preceding control interval, adjusts its video coding rate in accordance with morphogen concentrations, and then broadcasts a message containing information about its morphogen concentrations, stimulus E, attenuation coefficient A, and NIP (Notification of Inhibitor Peak) notification to its neighbors. We call the duration between the t-th control timing and the $t+1$-th control timing as the t-th control interval. We should note here that nodes behave in an asynchronous manner, although the control interval is identical among nodes. It means that timing of reaction-diffusion calculation and message emission is different among nodes.

The reaction-diffusion equation is identical among nodes. Since nodes are arranged in a grid layout and messages are exchanged at regular intervals, we spatially and temporally discretize Eqs. (1) and (2) as follows.

$$\begin{cases} u_t = u_{t-1} + \Delta t\Big\{F(u_{t-1}, v_{t-1}) - du_{t-1} + E(t-1) \\ \qquad + D_u \dfrac{(u^u_{t-1} + u^d_{t-1} + u^l_{t-1} + u^r_{t-1} - 4u_{t-1})}{\Delta h^2}\Big\} \\ v_t = v_{t-1} + \Delta t\Big\{G(u_{t-1}, v_{t-1}) - gv_{t-1} \\ \qquad + D_v \dfrac{(v^u_{t-1} + v^d_{t-1} + v^l_{t-1} + v^r_{t-1} - 4v_{t-1})}{\Delta h^2}\Big\}, \end{cases} \quad (5)$$

$$\begin{cases} F(u_{t-1},v_{t-1}) = \max\{0, \min\{au_{t-1} - bv_{t-1} - c, M\}\} \\ G(u_{t-1},v_{t-1}) = \max\{0, \min\{eu_{t-1} - hv_{t-1} - f, N\}\}. \end{cases} \quad (6)$$

At the t-th control timing, a node calculates the above reaction-diffusion equation to derive its morphogen concentrations u_t and v_t. A set of u^u_{t-1}, u^d_{t-1}, u^l_{t-1}, and u^r_{t-1} and a set of v^u_{t-1}, v^d_{t-1}, v^l_{t-1}, and v^r_{t-1} correspond to concentrations of activator and inhibitor of neighboring nodes in up, right, down, and left directions. These values are obtained from messages that a node received in the $t-1$-th control interval. If a node did not receive a message from a neighboring node in the $t-1$-th control interval, the latest value obtained in the preceding intervals is used instead. Δh and Δt correspond to the distance between nodes and the discrete step interval of time, respectively. There is the theoretical range of Δt for the equation reaches convergence and a stable pattern is formed.

$$0 < \Delta t < \min\{\frac{2}{d + 4D_u(\Delta x^{-2} + \Delta y^{-2})}, \frac{2}{g + 4D_v(\Delta x^{-2} + \Delta y^{-2})}\}. \quad (7)$$

If the degree of temporal discretization is not within this range, a pattern does not converge. $E(t-1)$ in Eq. (5) is the amount of stimulus which is determined at the t-th control timing, based on messages it received in the $t-1$-th control interval and the condition of a target if exists. The stimulus controls the distribution of morphogen concentrations, that is, a pattern. Usually, the amount of stimulus is zero. A node which detects a target in the $t-1$-th control interval appropriately sets E and A in accordance with the speed and direction of the target, so that a spot pattern centered at the node is generated. The stimulus diffuses to nodes in the direction of target movement so that they prepare for the future appearance of the target in their observation area as shown in Fig. 4. The attenuation coefficient A is used for

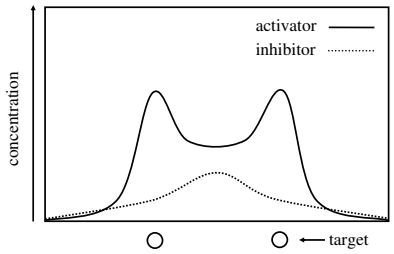

(a) Distribution of morphogen concentrations

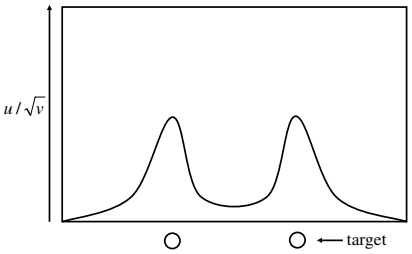

(b) Distribution of $u/\sqrt{v}$

Figure 5: Distribution of u, v, and $u/\sqrt{v}$ with closely located targets

this purpose. Details of stimulus determination and diffusion will be explained in subsection 3.2. NIP notification is used to regulate the amount of stimulus when two or more targets are closely located. Details of NIP will be given in subsection 3.3.

Once morphogen concentrations are derived, a node translates the concentrations to the video coding rate that it uses during the t-th control interval. As explained in Section 2, a spatial pattern generated by a reaction-diffusion model comes from the spatial heterogeneity in concentration of activator. However, an approach to directly map the concentration of activator to the video coding rate fails when two or more targets are close together. In Fig. 5(a), we illustrate the distribution of concentrations of morphogens. As can be seen, the region between two peaks of the concentration of activator has the high concentration of activator, because the region is activated by diffused activator while it is also inhibited by diffused inhibitor. If we set the video coding rate in proportional to the concentration of activator for example, regions inbetween closely located targets generate unnecessarily high-quality video data. Therefore, in our mechanism, by focusing on a phenomenon that the concentration of inhibitor is also high in the region as shown in Fig. 5(a), a node determines the video coding rate based on $u/\sqrt{v}$, whose distribution is illustrated in Fig. 5(b). If $v < 1$, then we set $u/\sqrt{v} = 0$, in order to avoid the divergence of $u/\sqrt{v}$. In the paper, we use the value $u/\sqrt{v}$ as the video coding rate.

3.2 Stimuli arrangement

In the reaction-diffusion equation, stimuli decide the position, shape, and size of spot patterns. When we set the stimulus high at a certain node, the concentration of activator becomes high at the node and a spot centered at the node emerges. To keep monitoring a moving target, cameras in the region to which the target is expected to move should use the sufficiently high coding rate for the future appearance (Fig. 4). Therefore, in our mechanism, a node detecting a moving target diffuses the stimulus to nodes in the moving direction.

If a node has a target in its observation area at the control timing, it sets the amount of stimulus E, the attenuation coefficient A, and the direction of diffusion. The node calculates the morphogen concentrations, set the video coding rate, and broadcasts a message containing this information.

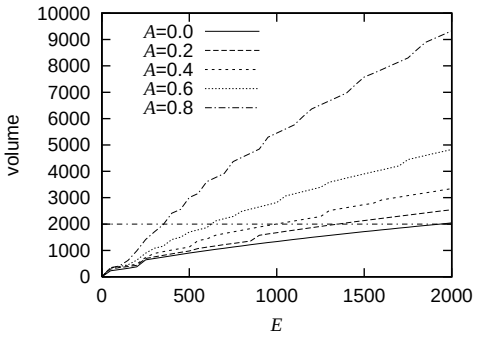

Figure 6: Relationship among A, E, volume of pattern

A node receiving a message first sees whether it is in the direction of the target movement. If not, it ignores the information. If the node should be prepared for the target, it first calculates the amount of stimulus E' from the informed E and A as $E' = A \times E$. This stimulus is used as $E(t-1)$ at the t-th control timing in calculating the morphogen concentrations. After the calculation, the information about the stimulus, including E', A, and the direction is further diffused to neighbor nodes by being embedded in a broadcast message. When a node receives multiple messages containing stimuli from neighbor nodes, it uses the sum of E' as $E(t-1)$.

The amount of stimulus E and the attenuation coefficient A are determined in accordance with the movement of target and the capacity of wireless channel. In Fig. 6, the relationship among E, A, and the volume of a generated pattern is shown for the case with a single target. The volume of a pattern is defined as,

$$v(E, A) = \sum_{(i,j)} u(i,j)/\sqrt{v(i,j)}. \quad (8)$$

$u(i,j)$ and $v(i,j)$ are the concentrations of activator and inhibitor at node (i,j) on a converged stable pattern, respectively. Since a node chooses the video coding rate depending on $u(t)/\sqrt{v(t)}$, the volume corresponds to the total amount of traffic generated by nodes in a spot. As shown in the figure, the volume $v(E, A)$ is almost in proportional to the stimulus E. As the attenuation coefficient A increases, the

Table 1: Setting for 10×10 nodes simulation

parameter	value	parameter	value
a	0.08	h	0.05
b	0.2	D_u	0.004
c	0.2	D_v	0.1
d	0.03	M	0.2
e	0.1	N	0.5
f	0.14	Δt	0.1
g	0.06	Δh	1

Table 2: Mapping from V to A and range of E

V (km/h)	A	Upper limit of E	Lower limit of E
$V = 0$	0.0	1960	830
$0 < V \leq 2$	0.2	1370	700
$2 < V \leq 4$	0.4	1010	440
$4 < V \leq 6$	0.6	620	390
$6 < V$	0.8	360	260

volume $v(E, A)$ increases for the same stimulus E. Since the attenuation coefficient A determines the range of stimulus diffusion, a node detecting a target first sets the attenuation coefficient A in accordance with the speed V of target. Then, the node determines the stimulus E to keep the total traffic at a certain volume from $v(E, A)$. For example, when the capacity of local wireless network is 2000 in volume and A is 0.4, E is set at 1010. The mappings from the network capacity to the volume and from the speed to the attenuation coefficient depend on the system conditions and application requirements.

3.3 Stimuli adjustment

With the mechanisms we explained so far in the paper, a desired spot pattern appears and each node generates video data with the appropriate quality in accordance with the location, speed, and direction of a moving target without knowing the complete information about the whole system. However, when two or more targets are located close together, the total amount of video traffic would exceed the network capacity in that area. As a consequence, the perceived video quality considerably deteriorates for loss and delay of video data. To tackle the problem, we additionally propose the stimuli adjustment mechanism.

A basic idea is as follows. When two or more targets are close together, spots centered at them overlap with each other. If a node can detect the overlap and inform to the nodes setting the stimuli, the amount of stimuli can be adjusted so that spots become small and apart from each other. As shown in Fig. 5(a), when two targets are closely located, both of concentrations of activator and inhibitor become high at the inbetween region. Especially, the concentration of inhibitor has a peak at the center. By using this phenomena, a node at the overlapping point detects the overlap.

At the control timing, a node compares the concentration of inhibitor of itself with those of neighboring nodes. If the concentration is the highest at the node and it does not have a target in its observation area, it sets the NIP notification in a message it broadcasts. Now, a node receives a message. If $u/\sqrt{v}$ of the node is higher than that of a node from which it received NIP, the node has the stimulus, or any neighboring node of the node has a target, it sets NIP in a broadcast message. As a consequence, NIP follows the gradient of $u/\sqrt{v}$ and diffused stimuli toward nodes having a target.

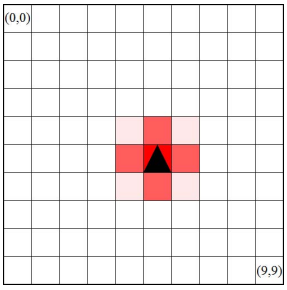

Figure 7: Distribution of morphogen concentrations with one stationary target

When a node having a target receives a message with NIP, it reduces the stimulus E as $E \times \alpha$ ($0<\alpha<1$). When the targets move apart from each other and the overlap disappears, the stimulus has to be increased. Therefore, a node having a target increases the stimulus as $E = E + \Delta e$, if it does not receive any NIP in the preceding control interval. The stimulus must be large enough to generate a pattern and smaller than the maximum to keep the volume. The range is determined from $v(E, A)$. For example, with $A = 0.4$, the range is from 440 to 1010.

4. SIMULATION EXPERIMENTS

In this section, we show results of simulation experiments to verify the effectiveness of our mechanism. One hundred nodes are arranged in a 10×10 grid with separation of 100 meters. Parameter setting for the reaction-diffusion equation is summarized in Table 1. For the stimuli adjustment, $\alpha = 0.999$ and $\Delta e = 1$ are used. We determine the relationship $v(E, A)$ from Fig. 6, which is obtained by preliminary experiments with one stationary node. Assuming that the capacity of wireless network is 2000 in volume, the mapping from the speed V to the attenuation coefficient A and the range of the stimulus E are summarized in Table 2. Initially, the morphogen concentrations are set at zero.

First, we consider a scenario where there is one stationary target ($V = 1$) at the location of (5,5) in the monitoring region ($0 \leq x \leq 9, 0 \leq y \leq 9$). Figure 7 illustrates the distribution of $u/\sqrt{v}$ when a pattern converges. In the figure, each square corresponds to a node. The darker the square is, the higher the video coding rate and $u/\sqrt{v}$ are. A triangle indicates the location and direction of a node. The node in the figure faces upwards. As shown in the figure, a spot pattern centered at the target is formed. Figure 8 shows the distribution of morphogen concentrations and $u/\sqrt{v}$ on a horizontal line $y = 5$. As shown in the figure, the concentration of activator and $u/\sqrt{v}$, that is, the video coding rate is the highest at the node having the target.

In a reaction-diffusion model, a pattern does not appear at once. Since calculation and communication require energy and time and adjustment of video coding rate must be performed in time to monitor a moving target, we have to consider the time required for pattern generation. Fig-

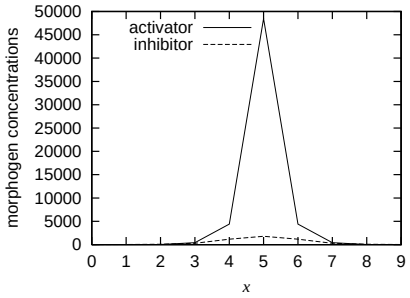

(a) Distribution of morphogen concentrations

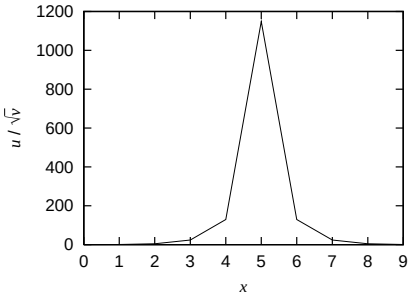

(b) Distribution of $u/\sqrt{v}$

Figure 8: Simulation results of one stationary target

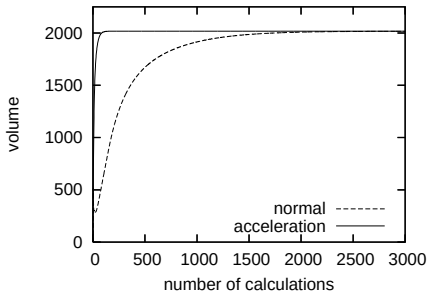

(a) Transition of volume

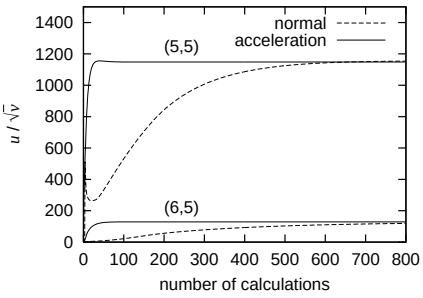

(b) Transition of $u/\sqrt{v}$

Figure 9: Transition of volume and video coding rate against number of calculations

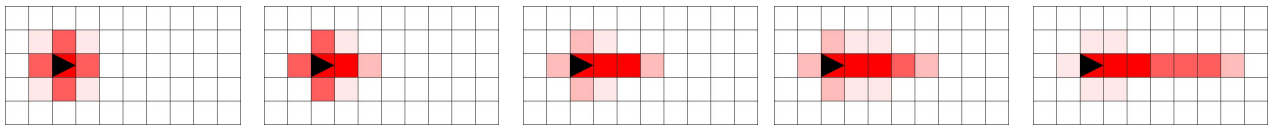

(a) $A = 0.0$ (b) $A = 0.2$ (c) $A = 0.4$ (d) $A = 0.6$ (e) $A = 0.8$

Figure 10: Generated patterns for a moving target

ure 9(a) shows the transition of the total volume against the number of calculations to show how fast a stable pattern emerges. For a pattern to converge, nodes have to calculate the reaction-diffusion equation and exchange messages about 2800 times as a line labeled as "normal" shows. To accelerate pattern generation, we introduce an acceleration method using a larger discrete step interval Δt [4]. A line labeled as "acceleration" in Fig. 9(a) shows the result of acceleration by setting Δt at 2.0, which is within the limit of $\Delta t = 2.32$ derived from Eq. (7). By the acceleration, the number of calculations is greatly reduced to 140. Now, assume that a target is moving at the speed of 4 km/h. A target passes across the observation area of 100 m $\times$ 100 m in 90 seconds. Since the control interval should be in an order of several seconds at least, the 140-times calculation is still too large to generate a pattern in time. However, it is not necessarily required for the whole pattern to converge from a practical point of view as far as a camera having a target generates the high-quality video data. Figure 9(b) shows the transition of $u/\sqrt{v}$ at a node detecting a target. For $u/\sqrt{v}$ to converge, the node needs to calculate the reaction-diffusion equation 85 times. However, as shown in the figure, the concentration drastically increases to the sufficiently high value in about 30-times calculations. As nodes exchange messages and calculate the reaction-diffusion equation, further nodes eventually adjust the video coding rate as shown in Fig. 9(b).

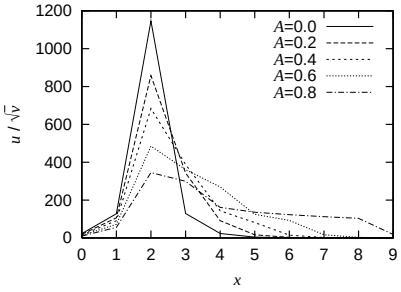

(a) Distribution of $u/\sqrt{v}$

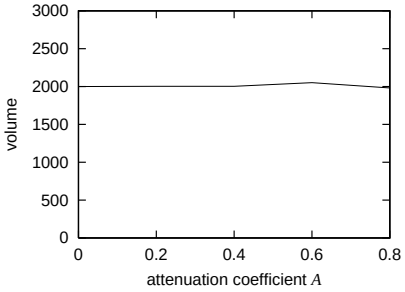

(b) Volume

Figure 11: Simulation results of one moving target

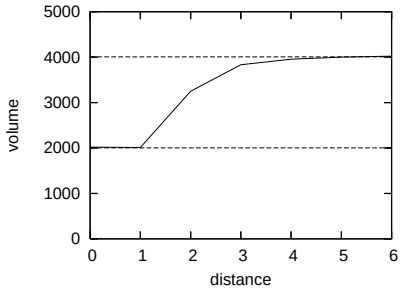

(a) Volume against target distance

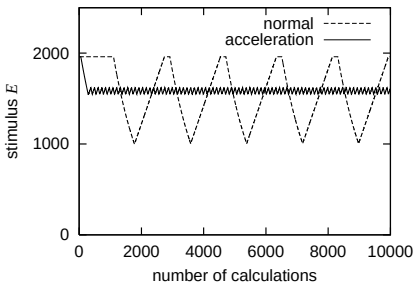

(b) Transition of stimulus

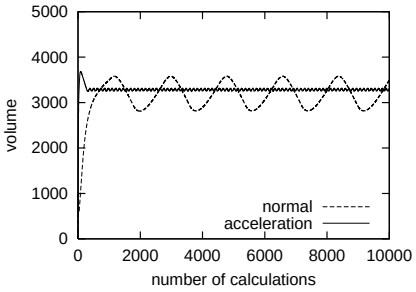

(c) Transition of volume

Figure 12: Simulation results of two stationary targets

A pattern is gradually generated from the center.

Next we set the speed of a stationary node at (2,5) as 1, 3, 5, and 7 km/h, which are mapped to A of 0.2, 0.4, 0.6, and 0.8, respectively. Figure 10 illustrates generated patterns. Figure 11(a) shows the distribution of $u/\sqrt{v}$ for the different attenuation coefficient on $y = 5$. As can be seen, as A, i.e., the speed of moving target, increases, the resultant pattern spreads wider and the height of peak becomes lower. As shown in Fig. 11(b), the total volume is kept constant at the given capacity even when the speed changes with our stimulus setting.

Then, to verify the effectiveness of our stimuli adjustment for closely located targets, we conduct simulation experiments with two stationary targets. Figure 12(a) shows the relationship among the distance between targets and the total volume of converged pattern. Two dashed lines correspond to the volume for the case of one stationary target (lower line) and its doubled amount (upper line), respectively. The distance of zero corresponds to the case of one stationary target. As shown in the figure, the total volume is suppressed when the distance between two targets is small. In cases of the distance of one and two, intermediate nodes detect the overlap, NIP is sent to the nodes detecting targets, and the stimuli are decreased. Once the stimuli become small enough, the two nodes begin to increase the stimuli again for not receiving NIP. As a result, the stimuli fluctuate as shown in Fig. 12(b), where the transition of stimulus at one of nodes having a target is depicted for the case of distance of two. It should be noted that the acceleration method also contributes to suppression of the oscillation. We see the same effect in the total volume as shown in Fig. 12(c). In the case of distance of three or more, spots centered at targets do not overlap with each other and NIP is not used.

Finally, we consider a scenario with multiple moving targets. Initially, targets which move to the random direction at the random speed from 0 to 8 km/h are located at randomly chosen nodes. At every control timing, a target changes the speed and direction with the probability of 0.005. The control interval is set at 2 seconds. At every $180/V$ control intervals, a moving target migrates to a neighboring node in the moving direction. Here, $180/V$ is the time required for a target moving at the speed of V km/h travels 100 meters. The discrete step Δt is set at 2.0.

Figure 13(a) depicts the transition of volume with three moving targets. Depending on the distance among targets and their speed and direction, the total volume dynamically changes. One reason that the total volume exceeds 6000, i.e., the triple of the volume of a single target, is that the high concentration of activator sometimes remains behind

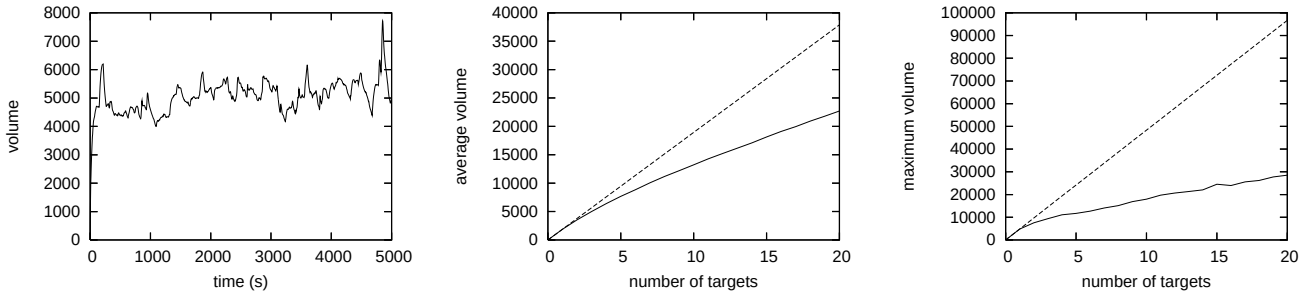

(a) Transition of volume with three moving targets

(b) Average volume against number of moving targets

(c) Maximum volume against number of moving targets

Figure 13: Simulation results of multiple moving targets

a fast moving target. The other reason is that suppression of stimulus E is too slow for closely located targets moving at the speed of more than 6 km/h. We need to accelerate pattern adaptation, but it is one of future works.

Figures 13(b) and 13(c) show the relationship among the number of targets and the average and maximum volume of generated patterns, respectively. The dashed lines stand for the product of the number of nodes and the value for one target. As shown in the figures, our mechanism suppresses the traffic volume much lower by reaction-diffusion based control.

Although results are not shown, we also conducted simulation experiments on a large-size network, where 2500 nodes are arranged in a 50×50 grid with separation of 100 meters. We verified that every node appropriately adjusts the video coding rate to monitor moving targets.

5. CONCLUSIONS

In this paper, we proposed a reaction-diffusion based autonomous control mechanism for camera sensor networks. In our mechanism, nodes periodically exchange information about the morphogen concentrations, calculate the reaction-diffusion equation, and adjust the video coding rate. By setting the stimulus at a node detecting a target and diffusing the stimulus, the video coding rate becomes high at a node with a target and nodes in the moving direction.

Although the effectiveness of the mechanism is verified through simulation experiments, we require further improvement. Since the video traffic is concentrated in the proximity of a target, there is the possibility of severe congestion in the local wireless network even with the coding rate control. We are going to incorporate control mechanisms of multiple layers with coding rate adjustment. For example, the video traffic can be dispersed by establishing multiple radial paths from the node having a target. The information about the degree of congestion can be taken into account in adjusting the video coding rate, as far as application requirements for the quality of video data are satisfied.

6. ACKNOWLEDGMENTS

We are very grateful to Assistant Professor Etsushi Nakaguchi for his valuable cooperation in our research. This research was partly supported by "Special Coordination Funds for Promoting Science and Technology: Yuragi Project" of the Ministry of Education, Culture, Sports, Science and Technology, Japan.

7. REFERENCES

[1] I. F. Akyildiz, T. Melodia, and K. R. Chowdhury. A Survey on Wireless Multimedia Sensor Networks. Computer Networks, 51(4):921–960, Mar. 2007.

[2] Y. Chen and T. C. Henderson. S-nets: Smart Sensor Networks. In Proceedings of International Symposium on Experimental Robotics, pages 85–94, Dec. 2000.

[3] M. Durvy and P. Thiran. Reaction-Diffusion Based Transmission Patterns for Ad Hoc Networks. In Proceedings of IEEE INFOCOM 2005, volume 3, pages 2195–2205, Mar. 2005.

[4] K. Hyodo, N. Wakamiya, E. Nakaguchi, M. Murata, Y. Kubo, and K. Yanagihara. Experiments and Considerations on Reaction-Diffusion based Pattern Generation in a Wireless Sensor Network. In Proceedings of 1st IEEE International Workshop: From Theory to Practice in Wireless Sensor Networks (t2pWSN 2007), Jun. 2007.

[5] T. Nakamura, N. Mine, E. Nakaguchi, A. Mochizuki, M. Yamamoto, K. Yashiro, C. Meno, and H. Hamada. Generation of Robust Left-Right Asymmetry in the Mouse Embryo Requires a Self-Enhancement and Lateral-Inhibition System. Developmental Cell, 11:495–504, Oct. 2006.

[6] A. M. Turing. The Chemical Basis of Morphogenesis. Royal Society of London Philosophical Transactions Series B, 237:37–72, Aug. 1952.

[7] A. Yoshida, K. Aoki, and S. Araki. Cooperative Control Based on Reaction-Diffusion Equation for Surveillance System. In Proceedings of Ninth International Conference on Knowledge-Based Intelligent Information and Engineering Systems, pages 533–539, Sep. 2005.